

## A NEW MODEL FOR THE CONTACT SURFACE WITH SOIL OF CIRCULAR ISOLATED FOOTINGS CONSIDERING THAT THE CONTACT SURFACE WORKS PARTIALLY UNDER COMPRESSION

SAMUEL SOTO-GARCIA<sup>1</sup>, ARNULFO LUÉVANOS-ROJAS<sup>1,\*</sup>  
JOSÉ DANIEL BARQUERO-CABRERO<sup>2</sup>, SANDRA LÓPEZ-CHAVARRÍA<sup>1</sup>  
MANUEL MEDINA-ELIZONDO<sup>1</sup>, OSCAR MARIO FARIAS-MONTEMAYOR<sup>1</sup>  
AND CARMELA MARTÍNEZ-AGUILAR<sup>1</sup>

<sup>1</sup>Instituto de Investigaciones Multidisciplinaria  
Facultad de Contaduría y Administración  
Universidad Autónoma de Coahuila, Unidad Torreón  
Blvd. Revolución 151 Ote. CP 27000, Torreón, Coahuila, México  
{samuelsoto; salopezc; mamedinae; oscarmariofarias; carmelamartinez}@uadec.edu.mx  
\*Corresponding author: arnulfoluevanos@uadec.edu.mx

<sup>2</sup>Institute for Long Life Learning IL3  
University of Barcelona  
Street Girona No. 24, CP 08010, Barcelona, Spain  
jd.barquero@eserp.com

Received January 2022; revised April 2022

**ABSTRACT.** *This paper presents a new model to obtain the most economical dimension of circular isolated footings considering that the contact surface works partially under compression (a part of the contact surface of the footing is subject to compression and the other part has zero pressure). The current model considers the entire area working under compression and is developed proposing different dimensions until complying with the biaxial bending equation (Minimum pressure must be equal to or greater than zero, and maximum pressure must be equal to or less than the allowable load capacity of the soil). Other authors present the equations to obtain the dimensions of the circular footing, but consider the total area working under compression. The methodology is developed as follows: The resultant moment “ $M_R$ ” is obtained, and by integration the axial load “ $P$ ” and the moment around of a  $X'$  axis “ $M_R$ ” are obtained. Numerical examples are presented to obtain the contact area of circular isolated footings under axial load and moments in two directions, and the results are compared with those of other authors. The results show that the new model is more economic and also more suitable to real conditions.*

**Keywords:** Circular isolated footings, Most economical dimension, Linear pressure distribution of the soil, Biaxial bending, Contact surface works partially to compression

**1. Introduction.** Foundations types are classified as deep and shallow according to their importance level: geometry function, soil behavior, structural function, and type of construction system. Shallow foundations can be of various types depending on their function: isolated footing, combined footing, strip footing, or mat foundation. The isolated footings are classified according to their geometry shape: rectangular, square and circular.

The plan dimensioning of the footings is usually carried out admitting a flat distribution for the stresses transmitted to the soil. This hypothesis is quite likely in highly

consolidated rocky or clayey and sandy soils and not so much for the latter when they are normally consolidated; in such a case, a parabolic stress distribution may be closer to reality. Taking the linear hypothesis into account, the calculation of stresses for a given footing and loads is direct and immediate in cases where soil detachment does not occur (i.e., when the entire base of the footing compresses the soil, with greater or less intensity), since then the stresses can be easily calculated from the system of linear equations that requires the balance between the actions on the base of the footing and the soil reaction (biaxial bending equation). This equation is invalid in the event that there is partial detachment of some area of the base, which is assumed to be traction. This occurs when the resultant is located outside the Central Nucleus, a well-known and delimited area.

The researchers who address the issue about the foundations dimensions are as the following: Khazaie and Amirshahkarami [1] developed constant computational models for small and large foundations under a uniform distributed load taking account of the interaction between the soil and the foundation, and it has been analyzed by ANSYS software, version 8.1; Jahanandish et al. [2] employed the stress level-based method of the zero extension lines to take account of the nonlinearity of the Mohr-Coulomb failure envelope to determinate of the bearing capacity factor “ $N\gamma$ ” in function of the foundation size; Luévanos-Rojas [3] presented a mathematical model to obtain the minimum dimensions of the rectangular isolated footings using optimization techniques; Vyacheslavovich and Adolfovich [4] investigated the stress-strain state of the foundation bed under the variously shaped footings and the foundation basis is featured by cohesive and non-cohesive soil; López-Chavarría et al. [5] employed the optimization techniques to obtain the minimum dimensions of the square isolated footings with eccentric load; López-Chavarría et al. [6] developed a model to obtain the minimum contact surface for the corner combined footings considering three columns, a corner column and two boundary columns. The analytical models have been presented to find the contact surface on the soil for square, rectangular and circular isolated footings subjected to an axial load and two moments in orthogonal directions (biaxial bending) [7-9]. A formulation is presented to obtain the dimensions of isolated footings under biaxial bending take account of the low concrete consumption [10]. A comparison is presented between the square, rectangular and circular footings in function of the contact surface with soil [11]. Other mathematical models have been studied to obtain the contact surface on the soil for rectangular, trapezoidal, strap and T-shaped combined footings subjected to an axial load and two moments in orthogonal directions in each column [12-15]. These models consider the contact surface subjected to compression totally.

Now, the researchers who address the issue about the foundations design are as the following: Luévanos-Rojas et al. [16] for rectangular isolated footings, Luévanos-Rojas [17] for circular isolated footings, Luévanos-Rojas [18] for boundary rectangular combined footings, Luévanos-Rojas [19] for boundary trapezoidal combined footings, Luévanos-Rojas et al. [20] for T-shaped combined footings, Yáñez-Palafox et al. [21] for strap combined footings, Luévanos-Rojas et al. [22] proposed the optimal design for rectangular isolated footings, and López-Chavarría et al. [23] developed a mathematical model for the design of square isolated footings with eccentric load. Also, these models consider the contact surface subjected to compression totally.

Several researches have developed mathematical models to determinate the stresses in the base of the rigid rectangular isolated footings with a linear soil pressure distribution considering that contact surface works partially to compression, such as Irlés-Más and Irlés-Más [24], Algin [25,26], Özmen [27], Bellos and Bakas [28,29], Aydogdu [30], and Girgin [31].

According to the literature review, the closest work is the dimensioning of circular isolated footings, but the surface area in contact with the soil is considered fully compressed. Therefore, there is no document with the current level of knowledge about the dimension of circular footings considering that contact surface works partially in compression.

This study shows an analytical model to obtain the dimension of the circular footings considering that contact area with the soil works partially to compression, i.e., a part of the contact area of the footing is subject to compression and the other there is no pressure and neither tensile. Other authors show the equations to obtain the dimensions of the circular footing, but consider the total area working under compression completely. Numerical examples are shown to find the contact area of circular footings under an axial load and moments in two directions, and the results are compared with those of other authors to observe the differences. In addition, this study presents the characteristics of the environment indicator related to quality of life [32].

The paper is organized as follows. Section 2 describes the formulation of the new model to obtain the dimension of the circular isolated footings considering that contact area with the soil works partially to compression. Section 2.1 shows when the resultant force is located inside the central nucleus. Section 2.2 presents when the resultant force is located outside the central nucleus. Section 3 shows the numerical problems applied by the new model for circular isolated footings. Section 4 presents the results. Section 5 shows the conclusions to complete the paper.

**2. Formulation of the New Model.** Figure 1 shows an axial load “ $P$ ” and two moments “ $M_x$  and  $M_y$ ” in orthogonal directions (biaxial bending) applied to a circular isolated footing.

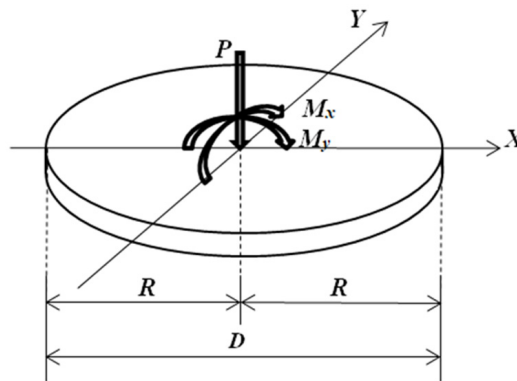


FIGURE 1. Load and two moments applied to a circular isolated footing

General equation for any type of footings subjected to biaxial bending is

$$\sigma = \frac{P}{A} + \frac{M_x y}{I_x} + \frac{M_y x}{I_y} \tag{1}$$

where  $\sigma$  is the soil pressure on the footing,  $A$  is the contact surface of the footing,  $P$  is the load applied at the center of gravity of the footing,  $M_x$  is the moment applied on the  $X$  axis,  $M_y$  is the moment applied on the  $Y$  axis,  $x$  is the distance in the  $X$  direction measured from the center of gravity to the fiber under study,  $y$  is the distance in  $Y$  direction measured from the center of gravity to the fiber under study,  $I_y$  is the moment of inertia around the  $Y$  axis and  $I_x$  is the moment of inertia around the  $X$  axis.

Now, to simplify the problem, the resultant moment “ $M_R$ ” is obtained from the two orthogonal moments “ $M_x$  and  $M_y$ ” and thus works with a single moment.

Figure 2 presents an axial load “ $P$ ” and a resultant moment “ $M_R$ ” of the two moments applied on the  $X$  and  $Y$  axes to a circular isolated footing, and it also shows the radius  $R$  and the diameter  $D$ .

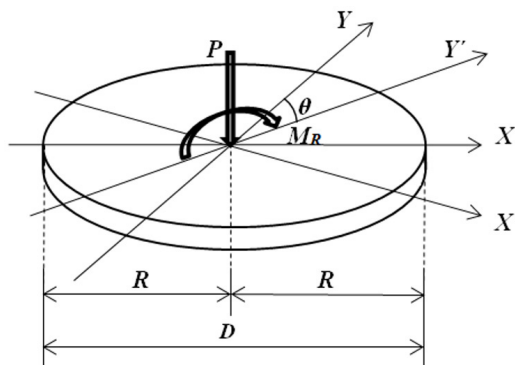


FIGURE 2. Load and a resultant moment applied to a circular isolated footing

The resultant moment “ $M_R$ ” is obtained as follows:

$$M_R = \sqrt{M_x^2 + M_y^2} \tag{2}$$

The inclination angle “ $\theta$ ” of the  $Y'$  axis with respect to the  $Y$  axis is

$$\cos \theta = \frac{M_x}{M_R} \rightarrow \theta = \arccos \left( \frac{M_x}{M_R} \right) \tag{3}$$

The soil pressure on the circular footing at any point by Equations (1) and (2) is obtained:

$$\sigma = \frac{P}{A} + \frac{M_R y'}{I_{x'}} \tag{4}$$

Substituting  $A = \pi R^2$  and  $I_{x'} = \pi R^4/4$  into Equation (4) is obtained:

$$\sigma = \frac{P}{\pi R^2} + \frac{4M_R y'}{\pi R^4} \tag{5}$$

Figure 3 shows the central nucleus of a circular footing (blue shaded area). If the resultant force is located inside the central nucleus, the entire area under the footing is subjected to compression. If the resultant force is located outside the central nucleus, a

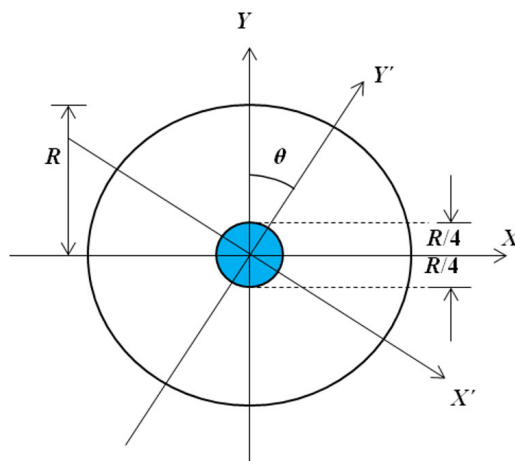


FIGURE 3. Central nucleus of a circular isolated footing

part of the area under of the footing is subjected to compression (this situation is well known).

The eccentricity  $e_R$  is obtained by the following equation:

$$e_R = \frac{M_R}{P} \tag{6}$$

**2.1. The resultant force is located inside the central nucleus, i.e.,  $e_R \leq R/4$ .** General equation for a circular footing is

$$\sigma = \frac{P}{\pi R^2} + \frac{4M_R y'}{\pi R^4} \leq \sigma_p \tag{7}$$

where  $\sigma_p$  is permissible load capacity of the soil.

Substituting  $y' = R$  into Equation (7) is obtained:

$$\sigma = \frac{P}{\pi R^2} + \frac{4M_R}{\pi R^3} \leq \sigma_p \tag{8}$$

If the minimum pressure is considered equal to zero by Equation (8), it can be expressed as follows:

$$R = \frac{4M_R}{P} \tag{9}$$

If the maximum pressure is considered equal to the permissible load capacity of the soil by Equation (8), it can be expressed as follows:

$$\sigma_p \pi R^3 - PR - 4M_R = 0 \tag{10}$$

Then, the value of  $R$  that must be considered to satisfy the two conditions is the greater value of Equations (9) and (10). This is the model proposed by Luévanos-Rojas [7].

**2.2. The resultant force is located outside the central nucleus, i.e.,  $e_R > R/4$ .** Figure 4 shows the pressure diagram, when the resultant force is located outside the central nucleus, i.e., the pressure is generated in a part of the contact surface of the footing.

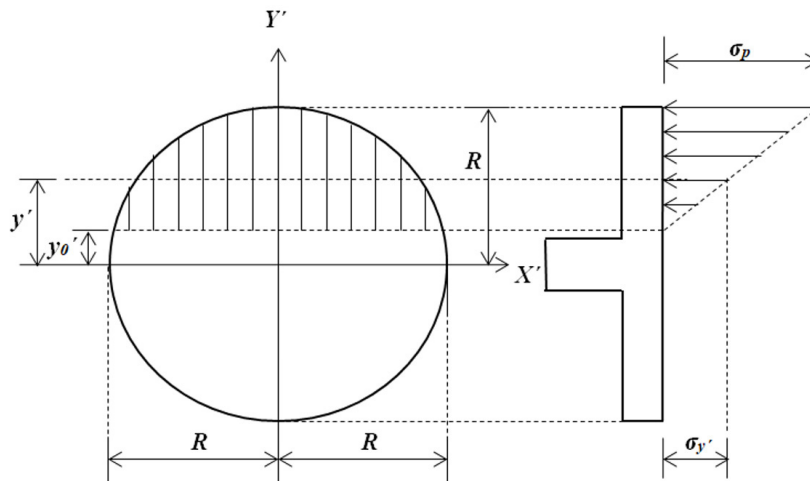


FIGURE 4. Pressure diagram of the circular isolated footing

The relationship between the maximum pressure “ $\sigma_p$ ” and the pressure at anywhere of the footing “ $\sigma_{y'}$ ” is found as follows:

$$\frac{\sigma_p}{R - y_0'} = \frac{\sigma_{y'}}{y' - y_0'} \tag{11}$$

By Equation (11), the pressure at anywhere of the circular footing is obtained:

$$\sigma_{y'} = \frac{\sigma_p(y' - y_0')}{R - y_0'} \quad (12)$$

Now, by integration the vertical load generated by the soil pressure is found, and the sum of forces acting on the footing is obtained through the following equation:

$$P = \int_{y_0'}^R \sigma_{y'} dA \quad (13)$$

where

$$dA = 2x' dy' \quad (14)$$

$$x' = \sqrt{R^2 - y'^2} \quad (15)$$

Substituting Equations (12), (14) and (15) into Equation (13) is obtained:

$$P = \frac{2\sigma_p}{R - y_0'} \int_{y_0'}^R (y' - y_0') \sqrt{R^2 - y'^2} dy' \quad (16)$$

Simplifying Equation (16) is obtained:

$$P = \frac{\sigma_p}{R - y_0'} \left[ \frac{(2R^2 + y_0'^2) \sqrt{R^2 - y_0'^2}}{3} + R^2 y_0' \arcsin \left( \frac{y_0'}{|R|} \right) - \frac{R y_0' \pi |R|}{2} \right] \quad (17)$$

Now, by integration the moment generated by the soil pressure is found, and the sum of moments acting on the footing is obtained through the following equation:

$$M_R = \int_{y_0'}^R \sigma_{y'} y' dA \quad (18)$$

Substituting Equations (12), (14) and (15) into Equation (18) is obtained:

$$M_R = \frac{2\sigma_p}{R - y_0'} \int_{y_0'}^R (y' - y_0') y' \sqrt{R^2 - y'^2} dy' \quad (19)$$

Simplifying Equation (19) is obtained:

$$M_R = -\frac{\sigma_p}{R - y_0'} \left[ \frac{y_0' (5R^2 - 2y_0'^2) \sqrt{R^2 - y_0'^2}}{12} + \frac{R^4}{4} \arcsin \left( \frac{y_0'}{|R|} \right) - \frac{R^3 \pi |R|}{8} \right] \quad (20)$$

Subsequently,  $\sigma_p$ ,  $P$  and  $M_R$  (known values) are substituted into Equations (17) and (20) to obtain  $R$  and  $y_0'$ .

Figure 5 presents the footing where the line crosses the circumference (pressure zero or neutral axis) to obtain the coordinates on the two types of axes.

The rotated coordinates ( $X'$ ,  $Y'$ ) are obtained as follows:

$$P_1' = \left( \sqrt{R^2 - y_0'^2}, y_0' \right) \quad (21)$$

$$P_2' = \left( -\sqrt{R^2 - y_0'^2}, y_0' \right) \quad (22)$$

The original coordinates ( $X$ ,  $Y$ ) are

$$P_1 = \left( y_0' \sin \theta + \sqrt{R^2 - y_0'^2} \cos \theta, y_0' \cos \theta - \sqrt{R^2 - y_0'^2} \sin \theta \right) \quad (23)$$

$$P_2 = \left( y_0' \sin \theta - \sqrt{R^2 - y_0'^2} \cos \theta, y_0' \cos \theta + \sqrt{R^2 - y_0'^2} \sin \theta \right) \quad (24)$$

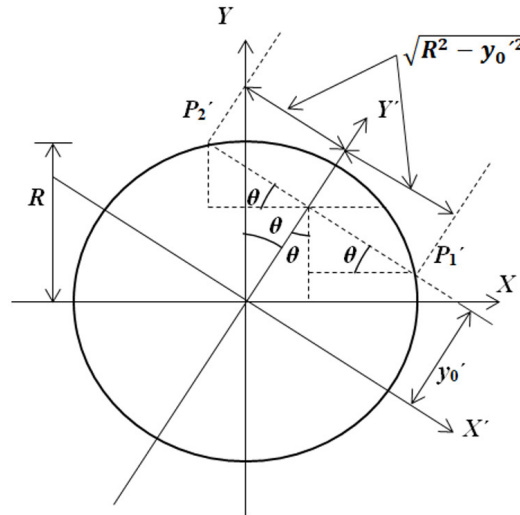


FIGURE 5. Coordinates on the two types of axes for the circular isolated footing

**3. Numerical Problems.** Tables present three cases for dimensioning of circular isolated footings, for the three cases  $P = 500$  kN and  $M_y = 100$  kN-m, and  $M_x = 300$  kN-m for the case 1,  $M_x = 200$  kN-m for the case 2,  $M_x = 150$  kN-m for the case 3, and each case presents four types of permissible load capacity of the soil of  $\sigma_p = 250, 200, 150, 100$  kN/m<sup>2</sup>, that are the same in all cases. The decrease in  $M_x$  is to observe the differences in the radius and area of the footing.

Table 1 shows the numerical problems of the new model for three cases of circular isolated footings. Substituting the values of  $\sigma_p, P$  and  $M_R$  into Equations (17) and (20)

TABLE 1. New model

$\sigma_p$ (kN/m <sup>2</sup> )	$R$ (m)		$e_R$ (m)	$R$ (m)	$y_0'$ (m)	$R$ (m)	$y_0'$ (m)	$\sigma_{max}$ (kN/m <sup>2</sup> )	$\sigma_{min}$ (kN/m <sup>2</sup> )
	By Eq. (9)	By Eq. (10)		By Eqs. (17) and (20)		Proposed			
Case 1: $P = 500$ kN, $M_y = 100$ kN-m, $M_x = 300$ kN-m, $M_R = 316.23$ kN-m									
250	2.53	1.35	0.63	1.41	-0.52	1.45	-0.59	227.24	0.00
200	2.53	1.47	0.63	1.51	-0.70	1.55	-0.76	185.63	0.00
150	2.53	1.64	0.63	1.67	-0.96	1.70	-1.01	141.97	0.00
100	2.53	1.92	0.63	1.93	-1.41	1.95	-1.44	97.30	0.00
Case 2: $P = 500$ kN, $M_y = 100$ kN-m, $M_x = 200$ kN-m, $M_R = 223.61$ kN-m									
250	1.79	1.25	0.45	1.26	-0.81	1.30	-0.88	228.27	0.00
200	1.79	1.36	0.45	1.36	-1.00	1.40	-1.06	186.84	0.00
150	1.79	1.52	0.45	1.52	-1.28	1.55	-1.33	143.08	0.00
100	1.79	1.79	0.45	1.79	-1.78	1.80	*	97.94	0.30
Case 3: $P = 500$ kN, $M_y = 100$ kN-m, $M_x = 150$ kN-m, $M_R = 180.28$ kN-m									
250	1.44	1.19	0.36	1.19	-0.96	1.20	-0.98	244.55	0.00
200	1.44	1.30	0.36	1.30	-1.16	1.30	-1.17	198.89	0.00
150	1.44	1.45	0.36	*	*	1.50	*	138.75	2.72
100	1.44	1.71	0.36	*	*	1.75	*	94.80	9.14

\*There is no value. This means that the entire area of the footing works in compression.

is obtained the values of  $R$  and  $y_0'$ . Subsequently, the value of  $R$  is considered a practical value and is substituted into Equations (17) and (20) to obtain the values of  $\sigma_p$  and  $y_0'$ . This procedure is used for when the resultant force is located outside the central nucleus ( $e_R > R/4$ ). For when the resultant force is located inside the central nucleus ( $e_R \leq R/4$ ) use Equations (9) and (10) by Luévanos-Rojas [8].

Table 2 presents the coordinates  $(X', Y')$  and the coordinates  $(X, Y)$  of the numerical problems for the new model. Substituting the values of  $R$  and  $y_0'$  into Equations (21) and (22) is obtained the coordinates  $(X', Y')$ . Now, substituting the values of  $R$ ,  $y_0'$  and  $\theta$  into Equations (23) and (24) is obtained the coordinates  $(X, Y)$ .

TABLE 2. Coordinates

$\sigma_p$ (kN/m <sup>2</sup> )	Coordinates $(X', Y')$				$\theta$ (Rad)	Coordinates $(X, Y)$			
	$P_1'$		$P_2'$			$P_1$		$P_2$	
	$x'$ (m)	$y'$ (m)	$x'$ (m)	$y'$ (m)		$x$ (m)	$y$ (m)	$x$ (m)	$y$ (m)
Case 1: $P = 500$ kN, $M_y = 100$ kN-m, $M_x = 300$ kN-m, $M_R = 316.23$ kN-m									
250	1.32	-0.59	-1.32	-0.59	0.32	1.07	-0.98	-1.44	-0.14
200	1.35	-0.76	-1.35	-0.76	0.32	1.04	-1.15	-1.52	-0.30
150	1.37	-1.01	-1.37	-1.01	0.32	0.98	-1.39	-1.62	-0.53
100	1.31	-1.44	-1.31	-1.44	0.32	0.79	-1.78	-1.70	-0.95
Case 2: $P = 500$ kN, $M_y = 100$ kN-m, $M_x = 200$ kN-m, $M_R = 223.61$ kN-m									
250	0.96	-0.88	-0.96	-0.88	0.46	0.47	-1.21	-1.25	-0.36
200	0.91	-1.06	-0.91	-1.06	0.46	0.35	-1.36	-1.29	-0.54
150	0.80	-1.33	-0.80	-1.33	0.46	0.12	-1.55	-1.30	-0.84
100	*	*	*	*	*	*	*	*	*
Case 3: $P = 500$ kN, $M_y = 100$ kN-m, $M_x = 150$ kN-m, $M_R = 180.28$ kN-m									
250	0.69	-0.98	-0.69	-0.98	0.59	0.03	-1.20	-1.12	-0.43
200	0.57	-1.17	-0.57	-1.17	0.59	-0.18	-1.29	-1.12	-0.66
150	*	*	*	*	*	*	*	*	*
100	*	*	*	*	*	*	*	*	*

\*There is no value. This means that the entire area of the footing works in compression.

**4. Results.** Table 1 presents the following: The radius is obtained by Equations (17) and (20) because it has an eccentricity  $e_R > R/4$  for the three cases, with exception of the case 2 for the permissible load capacity of the soil of  $\sigma_p = 100$  kN/m<sup>2</sup>, and of the case 3 for the permissible load capacity of the soil of  $\sigma_p = 150$  kN/m<sup>2</sup> and  $\sigma_p = 100$  kN/m<sup>2</sup>. This can be observed directly in the table where the minimum stress does not reach the value of zero. The results show that when the value of the permissible load capacity of the soil  $\sigma_p$  decreases, the radius  $R$  increases and the value of  $y_0'$  increases in absolute value.

Table 2 shows the following: The coordinates  $(X', Y')$  are obtained by Equations (21) and (22), and these are verified because the points 1 and 2 are symmetrical with respect to the  $Y'$  axis. The coordinates  $(X, Y)$  are obtained by Equations (23) and (24), and are verified by obtaining the radius by means of these coordinates. The results show that when the value of the permissible load capacity of the soil  $\sigma_p$  decreases, the coordinates  $(X, Y)$  of the points 1 and 2 decrease.

Table 3 shows the numerical problems for three cases of circular isolated footings of the model proposed by Luévanos-Rojas [8]. Substituting the values of  $\sigma_p$ ,  $P$  and  $M_R$  into

TABLE 3. Model proposed by Luévanos-Rojas [8]

$\sigma_p$ (kN/m <sup>2</sup> )	$R$ (m)			Stresses on the footing	
	By Eq. (9)	By Eq. (10)	Proposed	$\sigma_{\max}$ (kN/m <sup>2</sup> )	$\sigma_{\min}$ (kN/m <sup>2</sup> )
Case 1: $P = 500$ kN, $M_y = 100$ kN-m, $M_x = 300$ kN-m, $M_R = 316.23$ kN-m					
250	2.53	1.35	2.55	48.76	0.19
200	2.53	1.47	2.55	48.76	0.19
150	2.53	1.64	2.55	48.76	0.19
100	2.53	1.92	2.55	48.76	0.19
Case 2: $P = 500$ kN, $M_y = 100$ kN-m, $M_x = 200$ kN-m, $M_R = 223.61$ kN-m					
250	1.79	1.25	1.80	97.94	0.30
200	1.79	1.36	1.80	97.94	0.30
150	1.79	1.52	1.80	97.94	0.30
100	1.79	1.79	1.80	97.94	0.30
Case 3: $P = 500$ kN, $M_y = 100$ kN-m, $M_x = 150$ kN-m, $M_R = 180.28$ kN-m					
250	1.44	1.19	1.45	150.99	0.41
200	1.44	1.30	1.45	150.99	0.41
150	1.44	1.45	1.50	138.75	2.72
100	1.44	1.71	1.75	94.80	9.14

TABLE 4. Comparison of the NM and the MPLR

$\sigma_p$ (kN/m <sup>2</sup> )	Radius (m)			Area (m <sup>2</sup> )		
	NM	MPLR	MPLR/NM	NM	MPLR	MPLR/NM
Case 1: $P = 500$ kN, $M_y = 100$ kN-m, $M_x = 300$ kN-m, $M_R = 316.23$ kN-m						
250	1.45	2.55	1.76	6.61	20.43	3.09
200	1.55	2.55	1.65	7.55	20.43	2.71
150	1.70	2.55	1.50	9.08	20.43	2.25
100	1.95	2.55	1.31	11.95	20.43	1.71
Case 2: $P = 500$ kN, $M_y = 100$ kN-m, $M_x = 200$ kN-m, $M_R = 223.61$ kN-m						
250	1.30	1.80	1.38	5.31	10.18	1.92
200	1.40	1.80	1.29	6.16	10.18	1.65
150	1.55	1.80	1.16	7.55	10.18	1.35
100	1.80	1.80	1.00	10.18	10.18	1.00
Case 3: $P = 500$ kN, $M_y = 100$ kN-m, $M_x = 150$ kN-m, $M_R = 180.28$ kN-m						
250	1.20	1.45	1.21	4.52	6.61	1.46
200	1.30	1.45	1.12	5.31	6.61	1.24
150	1.50	1.50	1.00	7.07	7.07	1.00
100	1.75	1.75	1.00	9.62	9.62	1.00

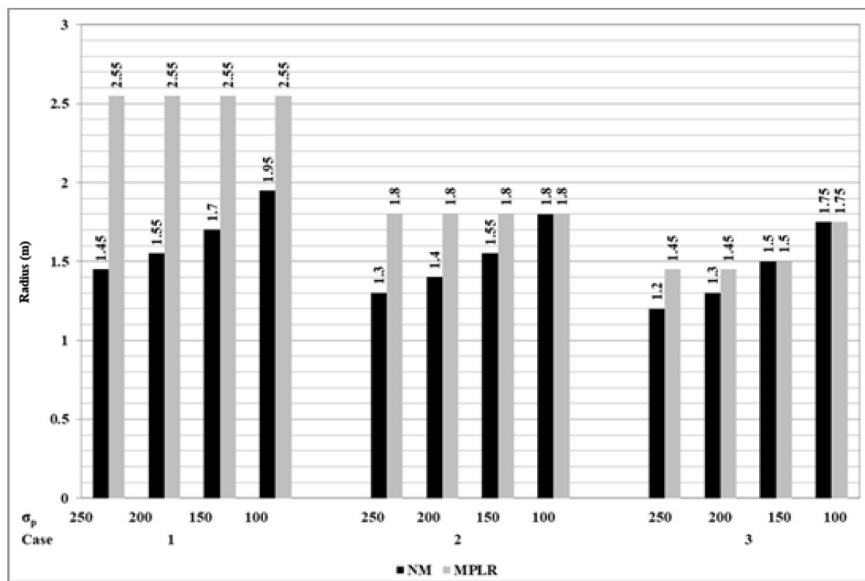
Equations (9) and (10) the value of  $R$  is obtained, and the largest is taken as the proposed radius.

Table 4 shows the comparison of the two models to observe the advantages of the new model (NM) against the model proposed by Luévanos-Rojas (MPLR) [8].

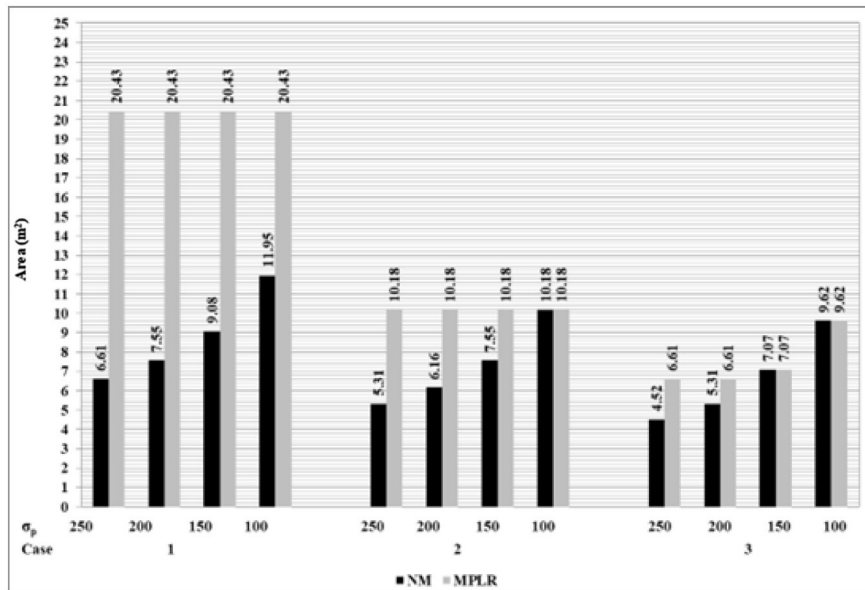
Table 3 presents the following: The radius is obtained by Equations (9) and (10), and the radius  $R$  is governed by Equation (9) for all the cases, with exception of the case 2 for the permissible load capacity of the soil of  $\sigma_p = 150 \text{ kN/m}^2$ , and of the case 3 for the permissible load capacity of the soil of  $\sigma_p = 150 \text{ kN/m}^2$  and  $\sigma_p = 100 \text{ kN/m}^2$  which is governed by Equation (10). This can be observed directly in the table where the maximum stress does not reach the value of the permissible load capacity of the soil  $\sigma_p$ .

Table 4 shows the following: The radius is obtained by Equations (17) and (20) for the new model and by Equations (9) and (10) for the model proposed by Luévanos-Rojas [8], and it is clearly observed that the new model presents smaller radius and smaller contact area with respect to the model proposed by Luévanos-Rojas [8].

Figure 6 shows the comparison between the two models in terms of radii and areas of the footings.



(a) Radius



(b) Area

FIGURE 6. Comparison between the two models

In Figures 6(a) and 6(b), the following are observed: When the permissible load capacity of the soil decreases, the difference between the two models is smaller, and in the cases that present the same value, it is because the area of the footing works completely in compression.

**5. Conclusions.** This paper presents a mathematical model of circular isolated footings to determine the radius and the position where stresses are zero in an elastic soil for an eccentrically loaded circular footing, assuming a linear pressure distribution of the soil.

The model consists of calculating the radius and the position where stresses are zero of a circular isolated footing subjected to biaxial bending, and the solution is obtained by solving the system of two equations that is generated by the balance of axial load and resultant moment, subsequently the radius is adjusted, and now the two equation systems are solved to obtain the position where stresses are zero and the maximum stress to verify if the maximum stress is less than the permissible load capacity of the soil.

The main contributions of this document are as the following.

1) The new model shows a significant reduction in the radius and in the contact area on the soil with respect to the model proposed by Luévanos-Rojas [8], if the resultant force is located outside the central nucleus ( $e_R = M_R/P > R/4$ ), i.e., when the moment  $M_R$  increases, the difference will be greater.

2) The new model shows an important advantage over any other model because it considers the contact area with the soil working partially to the compression, i.e., a part of the contact surface of the footing is subject to compression and for the other there is no pressure and neither tensile.

The new model presented in this document to obtain radius of the circular isolated footings subjected to an axial load and moment in two orthogonal directions due to the column, also it can be applied to an axial load, and an axial load and moment in a direction.

This study presents a robust and effective solution applied only to finding the radius of the circular isolated footings resting on elastic soil, which meet expression of the biaxial bending, i.e., the variation of the pressure is linear.

The suggestions for the next research are as follows:

1) Contact surface on the soil for the combined footing (rectangular, trapezoidal, corner and T-shaped) with the soil working partially under compression;

2) When totally cohesive soils (clay soils) and/or totally granular soils (sandy soils) are presented, the pressure diagram is different, because the pressure is not linear as it presented herein.

**Acknowledgment.** The research described in this work was funded by the Instituto de Investigaciones Multidisciplinaria of the Facultad de Contaduría y Administración of the Universidad Autónoma de Coahuila. The authors also gratefully acknowledge the helpful comments and suggestions of the reviewers, which have improved the presentation.

## REFERENCES

- [1] J. Khazaie and S. A. Amirshahkarami, Numerical analysis of interaction between earth and large foundations regarding size effect, *Journal of Applied Sciences*, vol.9, no.6, pp.1036-1045, 2009.
- [2] M. Jahanandish, M. Veiskarami and A. Ghahramani, Effect of foundation size and roughness on the bearing capacity factor,  $N_\gamma$ , by stress level-based ZEL method, *Arabian Journal for Science and Engineering*, vol.37, no.7, pp.1817-1831, 2012.
- [3] A. Luévanos-Rojas, A new approach for dimensioning of rectangular footings using optimization techniques, *ICIC Express Letters, Part B: Applications*, vol.6, no.11, pp.3141-3146, 2015.

- [4] G. A. Vyacheslavovich and B. L. Adolfovich, Influence of the form and size of the isolated foundations on the stress-strain state of the soil base, *Journal of Applied Engineering Science*, vol.14, no.1, pp.28-35, 2016.
- [5] S. López-Chavarría, A. Luévanos-Rojas and M. Medina-Elizondo, A mathematical model for dimensioning of square isolated footings using optimization techniques: General case, *International Journal of Innovative Computing, Information and Control*, vol.13, no.1, pp.67-74, 2017.
- [6] S. López-Chavarría, A. Luévanos-Rojas and M. Medina-Elizondo, Optimal dimensioning for the corner combined footings, *Advances in Computational Design*, vol.2, no.2, pp.169-183, 2017.
- [7] A. Luévanos-Rojas, A mathematical model for dimensioning of footings square, *International Review of Civil Engineering*, vol.3, no.4, pp.346-350, 2012.
- [8] A. Luévanos-Rojas, A mathematical model for the dimensioning of circular footings, *Far East Journal of Mathematical Sciences*, vol.71, no.2, pp.357-367, 2012.
- [9] A. Luévanos-Rojas, A mathematical model for dimensioning of footings rectangular, *ICIC Express Letters, Part B: Applications*, vol.4, no.2, pp.269-274, 2013.
- [10] W. L. de França Filho, R. C. Carvalho, A. L. Christoforo and F. A. R. Lahr, Dimensioning of isolated footing submitted to the under biaxial bending considering the low concrete consumption, *International Journal of Materials Engineering*, vol.7, no.1, pp.1-11, 2017.
- [11] A. Luévanos-Rojas, A comparative study for dimensioning of footings with respect to the contact surface on soil, *International Journal of Innovative Computing, Information and Control*, vol.10, no.4, pp.1313-1326, 2014.
- [12] A. Luévanos-Rojas, A new mathematical model for dimensioning of the boundary trapezoidal combined footings, *International Journal of Innovative Computing, Information and Control*, vol.11, no.4, pp.1269-1279, 2015.
- [13] A. Luévanos-Rojas, A mathematical model for the dimensioning of combined footings of rectangular shape, *Revista Técnica de la Facultad de Ingeniería Universidad del Zulia*, vol.39, no.1, pp.3-9, 2016.
- [14] A. Luévanos-Rojas, S. López-Chavarría and M. Medina-Elizondo, A new model for T-shaped combined footings Part I: Optimal dimensioning, *Geomechanics and Engineering*, vol.14, no.1, pp.51-60, 2018.
- [15] G. Aguilera-Mancilla, A. Luévanos-Rojas, S. López-Chavarría and M. Medina-Elizondo, Modeling for the strap combined footings Part I: Optimal dimensioning, *Steel and Composite Structures*, vol.30, no.2, pp.97-108, 2019.
- [16] A. Luévanos-Rojas, J. G. Faudoa-Herrera, R. A. Andrade-Vallejo and M. A. Cano-Alvarez, Design of isolated footings of rectangular form using a new model, *International Journal of Innovative Computing, Information and Control*, vol.9, no.10, pp.4001-4022, 2013.
- [17] A. Luévanos-Rojas, Design of isolated footings of circular form using a new model, *Structural Engineering and Mechanics*, vol.52, no.4, pp.767-786, 2014.
- [18] A. Luévanos-Rojas, Design of boundary combined footings of rectangular shape using a new model, *DYNA Colombia*, vol.81, no.188, pp.199-208, 2014.
- [19] A. Luévanos-Rojas, Design of boundary combined footings of trapezoidal form using a new model, *Structural Engineering and Mechanics*, vol.56, no.5, pp.745-765, 2015.
- [20] A. Luévanos-Rojas, S. López-Chavarría and M. Medina-Elizondo, A new model for T-shaped combined footings Part II: Mathematical model for design, *Geomechanics and Engineering*, vol.14, no.1, pp.61-69, 2018.
- [21] J. A. Yáñez-Palafox, A. Luévanos-Rojas, S. López-Chavarría and M. Medina-Elizondo, Modeling for the strap combined footings Part II: Mathematical model for design, *Steel and Composite Structures*, vol.30, no.2, pp.109-217, 2019.
- [22] A. Luévanos-Rojas, S. López-Chavarría and M. Medina-Elizondo, Optimal design for rectangular isolated footings using the real soil pressure, *Ingeniería e Investigación*, vol.37, no.2, pp.25-33, 2017.
- [23] S. López-Chavarría, A. Luévanos-Rojas and M. Medina-Elizondo, A new mathematical model for design of square isolated footings for general case, *International Journal of Innovative Computing, Information and Control*, vol.13, no.4, pp.1149-1168, 2017.
- [24] R. Irles-Más and F. Irles-Más, Analytical alternative to stress determination under rectangular footings with biaxial bending and partial debonding, *Informes de la Construcción*, vol.44, no.419, pp.77-90, 1992.
- [25] H. M. Algin, Stresses from linearly distributed pressures over rectangular areas, *International Journal for Numerical Analytical Methods in Geomechanics*, vol.24, no.8, pp.681-692, 2000.
- [26] H. M. Algin, Practical formula for dimensioning a rectangular footing, *Engineering Structures*, vol.29, no.6, pp.1128-1134, 2007.

- [27] G. Özmen, Determination of base stresses in rectangular footings under biaxial bending, *Teknik Dergi Digest*, vol.22, no.4, pp.1519-1535, 2011.
- [28] J. Bellos and N. P. Bakas, High computational efficiency through generic analytical formulation for linear soil pressure distribution of rigid spread rectangular footings, *Proc. of the 7th European Congress on Computational Methods in Applied Sciences and Engineering*, Crete Island, Greece, 2016.
- [29] J. Bellos and N. P. Bakas, Complete analytical solution for linear soil pressure distribution under rigid rectangular spread footings, *International Journal of Geomechanics*, vol.17, no.7, [https://doi.org/10.1061/\(ASCE\)GM.1943-5622.0000874](https://doi.org/10.1061/(ASCE)GM.1943-5622.0000874), 2017.
- [30] I. Aydogdu, New iterative method to calculate base stress of footings under biaxial bending, *International Journal of Engineering & Applied Sciences (IJEAS)*, vol.8, no.4, pp.40-48, 2016.
- [31] K. Girgin, Simplified formulations for the determination of rotational spring constants in rigid spread footings resting on tensionless soil, *Journal of Civil Engineering and Management*, vol.23, no.4, pp.464-474, 2017.
- [32] T. Nakashima and Y. Hirano, The features of indicator of the environment-related QOL (Quality of Life), *ICIC Express Letters, Part B: Applications*, vol.10, no.7, pp.613-618, 2019.

## Author Biography



**Samuel Soto-Garcia** received Industrial Engineering (2012) and Master in Industrial Engineering (2016) from the Instituto Tecnológico de la Laguna, and the degree of Doctor in Administration and Senior Management (2021) from the Facultad de Contaduría y Administración of the Universidad Autónoma de Coahuila. His research interests are mathematical models applied to Engineering and Administration.



**Arnulfo Luévanos-Rojas** received Civil Engineering (1981), Master in Science with Specialization in Structures (1983), Master in Science with Specialization in Planning and Construction of Works (2000), Master in Administration (2004), and Doctor in Engineering with Specialization in Planning Systems and Construction (2009). He was professor and researcher of the Facultad de Ingeniería, Ciencias y Arquitectura, Gomez Palacio Campus of the Universidad Juarez del Estado de Durango from since 2006 to 2015, and of the Facultad de Contaduría y Administración, Torreón campus of the Universidad Autónoma de Coahuila since 2015 to date. He has published more than 100 papers in journals indexed in the Web of Science. His research interests are mathematical models applied to Engineering and Administration. He is member of the National System of Researchers of Mexico.



**José Daniel Barquero-Cabrero** is doctor in the area of Economic, Legal and Social Sciences from the Universidad Internacional de Cataluña; Universidad Camilo José Cela de Madrid, Universitat Oberta de Catalunya, Universidad Autónoma de Coahuila de México and interuniversity by the Universities of Málaga, Huelva, Cádiz y Sevilla. He is also a Chartered Economist no. 13,049. He has been awarded for his contributions to the academic world with the title of doctor honoris causa by universities in America, Europe, Asia and Africa. He was awarded by the Government of Spain, Ministry of Foreign Affairs and Cooperation, the Commendation of the Order of Civil Merit. He was awarded by the European Development Foundation the European Cross in Gold. His research interests are mathematical models applied to Engineering and Administration.



**Sandra López-Chavarría** received the Master's degree in Administration and Senior Management, and the degree of Doctor in Administration and Senior Management from the Facultad de Contaduría y Administración of the Universidad Autónoma de Coahuila. She is the general coordinator of the Torreón campus of the Universidad Autónoma de Coahuila. She is professor and researcher for the Facultad de Contaduría y Administración, Torreón campus of the Universidad Autónoma de Coahuila. Her research interests are mathematical models applied to Engineering and Administration. She is member of the National System of Researchers of Mexico.



**Manuel Medina-Elizondo** received Master in Administration, Master in Management Science and Innovation, Doctor in Administration Sciences from the Universidad Nacional Autónoma de México, and Doctor in Administration from the Universidad de Newport of the State of California, U.S.A. He is current Chairman of the Delegation of Mexico's Superior Council of Doctors and Doctors Honoris Causa. He is professor, researcher, and General Coordinator of Research and Postgraduate of the Facultad de Contaduría y Administración, Torreón campus of the Universidad Autónoma de Coahuila. He has published more than 80 papers, and 15 books. His research interests are mathematical models applied to Engineering and Administration.



**Oscar Mario Farias-Montemayor** received industrial and systems engineering (2007), Master in Administration and leadership (1998) from the Universidad Autónoma del Noreste, and the degree of Doctor in Administration and Senior Management (2018) from the Facultad de Contaduría y Administración of the Universidad Autónoma de Coahuila. He is professor and researcher of the Facultad de Contaduría y Administración, Torreón campus of the Universidad Autónoma de Coahuila. Her research interests are mathematical models applied to Engineering and Administration.



**Carmela Martínez-Aguilar** received the Master's degree in Administration and Senior Management (2012) and the degree of Doctor in Administration and Senior Management (2022) from the Facultad de Contaduría y Administración of the Universidad Autónoma de Coahuila. She is professor and researcher of the Facultad de Contaduría y Administración, Torreón campus of the Universidad Autónoma de Coahuila. Her research interests are mathematical models applied to Administration.